

# Three-body recombination at finite energy within an optical model

P. K. Sørensen, D. V. Fedorov, A. S. Jensen and N. T. Zinner

*Department of Physics and Astronomy - Aarhus University,  
Ny Munkegade, bygn. 1520, DK-8000 Århus C, Denmark*

We investigate three-boson recombination of equal mass systems as function of (negative) scattering length, mass, finite energy, and finite temperature. An optical model with an imaginary potential at short distance reproduces experimental recombination data and allows us to provide a simple parametrization of the recombination rate as function of scattering length and energy. Using the two-body van der Waals length as unit we find that the imaginary potential range and also the potential depth agree to within thirty percent for Lithium and Cesium atoms. As opposed to recent studies suggesting universality of the threshold for bound state formation, our results suggest that the recombination process itself could have universal features.

The quantum mechanical three-body problem has a long and rich history. A milestone that has spurred great interest came in the early 1970ties when Efimov [1] found that three bosonic particles with short-range interactions can have an infinite number of three-body bound states when each two-body subsystem has a bound state with exactly zero binding energy. This intriguing possibility was pursued for many years in the context of nuclear physics [2–4], but its first experimental signature came using an ultra cold atomic gas of Cesium atoms in 2006 [5]. The use of tunable atomic interactions through the principle of Feshbach resonance [6] has enabled the study of these so-called Efimov three-body states in a number of different atomic alkali systems at low temperature [8–24]. While Efimov states are intrinsically low-energy spatially extended so-called universal states, the overall energy scale was previously believed to be given by short-range physics through a so-called three-body parameter,  $\Lambda$  [4]. A highly suggestive relation between  $\Lambda$  and the inter-atomic two-body van der Waals interactions was nevertheless recently suggested [25, 26]. A number of theoretical papers linking the short- and long-range energy scales of universal three-body physics soon followed [27–31] that hit at a universal short-range barrier in the effective three-body potential determined solely by parameters of the two-body inter-atomic potential. This has been interpreted as universality of the three-body parameter itself.

Here we present an entirely different approach to the problem of universality of three-body physics. The universality suggested in Ref. [25] was found in a region of parameter space where there are no weakly-bound two-body subsystems. There the observed recombination loss which is the most common signature of Efimov states takes place at short distance through decay into deeply bound two-body molecular states [4]. The problem then becomes how to match the long-distance universal three-body behaviour to a short-distance region capable of describing absorption due to three-body loss. In the present paper we construct a physically transparent model that uses a minimal number of parameters and does *not* require any short-range barrier. Instead we employ an

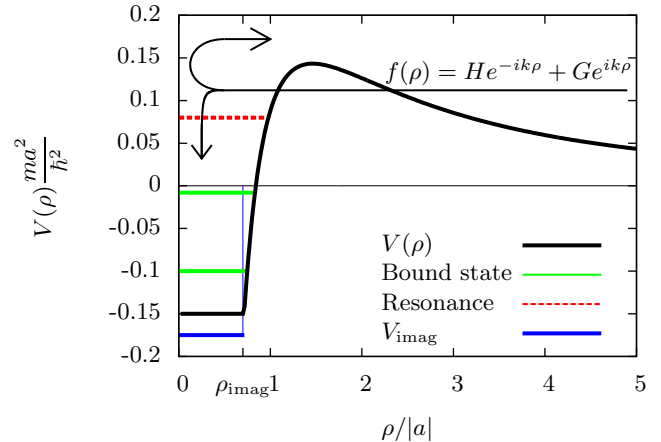


Fig. 1: Three-body model potential for negative scattering length  $a$  as function of hyperradius  $\rho$ . The actual  $\rho_{\text{imag}}$  used in calculations is much smaller than illustrated. The potential drops as  $1/\rho^2$  at large distances and has a constant (complex) value for  $\rho < \rho_{\text{imag}}$ . The split arrow indicates that amplitude is both reflected and absorbed via the complex potential. Green lines illustrate bound states in the potential while the green dashed line indicates a resonance.

imaginary potential inspired by optical models used in other areas of physics.

In Fig. 1 we show the effective potential for the three-body system. At long-distance there is a repulsive inverse-square which is separated by a barrier from an attractive inverse-square at intermediate distance, and at short distance an imaginary potential. The short-distance part may then be related to the two-body scale at which the decay to deeply bound states occurs. Below we show that this type of model describes experimental data for loss rates at different collision energies and/or finite temperatures extremely well. In addition, we demonstrate that when the imaginary part of the potential causing the loss is implemented in a (small) region of space the decay parameter,  $\gamma$ , depends on both scattering length,  $a$ , and on the collision energy. It also shows resonant features that obey appropriate Efimov scaling

relations. This is in contrast to many previous models [32–35] where an analogous parameter (typically denoted  $\eta$ ) is either found to be or assumed to be independent of energy and  $a$ .

A system of three bosonic particles of equal mass  $m$  at position  $\mathbf{r}_i$ ,  $\mathbf{r}_j$  and  $\mathbf{r}_k$  is treated using hyperspherical coordinates defined by  $\mathbf{x}_i = (\mathbf{r}_j - \mathbf{r}_k)/\sqrt{2}$  and  $\mathbf{y}_i = \sqrt{\frac{2}{3}}(\mathbf{r}_i - (\mathbf{r}_j + \mathbf{r}_k)/2)$ , where the Jacobi indices  $\{i, j, k\}$  are cyclic permutations of  $\{1, 2, 3\}$ . The hyper-radius  $\rho^2 = |\mathbf{x}_i|^2 + |\mathbf{y}_i|^2$  is independent of the choice of index. One hyperangle is defined as  $\alpha_i = \tan^{-1} \frac{|\mathbf{x}_i|}{|\mathbf{y}_i|}$  and the remaining four by the directions of  $\mathbf{x}_i$  and  $\mathbf{y}_i$ . We use the hyperspherical adiabatic approximation, the Faddeev decomposition and zero-range potentials to describe the interactions between the atoms. All methods are documented in detail in Ref. [36]. This yields a hyperradial differential equation

$$\left(-\frac{d^2}{d\rho^2} + \frac{\nu^2(\rho) - 1/4}{\rho^2} - \frac{2mE}{\hbar^2}\right) f(\rho) = 0, \quad (1)$$

where  $\nu(\rho)$  is determined implicitly by

$$\frac{\nu \cos\left(\frac{\nu\pi}{2}\right) - \frac{8}{\sqrt{3}} \sin\left(\frac{\nu\pi}{6}\right)}{\sin\left(\frac{\nu\pi}{2}\right)} = \sqrt{2} \frac{\rho}{a}, \quad (2)$$

where  $a$  is the common scattering length between each pair of particles. For negative scattering lengths the potential  $V(\rho) = \frac{\nu^2(\rho) - 1/4}{\rho^2}$  has a barrier region which the wave-function must penetrate, see Fig. 1. The limits of  $\nu^2$  is 4 and  $-1.012$  for large and small  $\rho$ , respectively. The potential is zero when  $\nu = 1/2$  corresponding to  $\rho = 0.84a$ , and the barrier maximum is at  $\rho = 1.46a$  with the peak height  $E_B(a) = 0.143\hbar^2/(ma^2)$ . The divergence due to  $1/\rho^2$  as  $\rho$  vanishes provides the Efimov scaling of 22.7 for bound or resonance states at zero energy. We select the range of these three-body states by continuing the real potential as a constant with the same value between 0 and the cut-off  $\rho_{\text{imag}}$ . Furthermore, we add a constant short-range imaginary potential,  $V(\rho < \rho_{\text{imag}}) = V_{\text{imag}}$ , acting as a probability sink which models recombination to deep dimers, see Fig. 1. This is in stark contrast to the usual regularization cut-off method where the potential is set to infinity for  $\rho$ -values below some small cut-off value. This is important as it means that we do not use repulsive core at short distance as in many previous studies. In this paper we use a completely different strategy where we avoid a three-body cut-off but obtain a model for the loss that matches experimental data as we show below. The imaginary potential reflects short-distance two-body effects coming from the neglected Hilbert space with deeply bound dimers. This can formally be done through Feshbach reaction theory that facilitates reduction to a smaller active Hilbert space.

We calculate the three-body recombination rate  $\alpha_{\text{rec}}$  for negative scattering length using the radial equation Eq.(1) directly. The rate is defined as  $\dot{n} = -\alpha_{\text{rec}}n^3$  where  $n$  is the particle density. At large hyperradii the wavefunction is decomposed into incoming and outgoing plane waves  $f(\rho) = He^{-ik\rho} + Ge^{ik\rho}$  with  $k^2 = 2mE/\hbar^2$ . The probability of recombination is simply  $R = 1 - |G/H|^2$ . The loss of probability is quantified using a complex phase-shift between incoming and outgoing waves

$$G = e^{2i(\theta+i\gamma)} H. \quad (3)$$

The recombination probability,  $R$ , is proportional to the absorption cross section and we write  $R = 1 - e^{-4\gamma}$  where  $\gamma$  is the decay parameter. The recombination rate is obtained using the method of Ref. [36], and given by

$$\alpha_{\text{rec}} = 4(2\pi)^2 3\sqrt{3} \frac{\hbar^5}{m^3} \frac{R}{E^2}. \quad (4)$$

This is obtained after dividing  $R$  by  $E^2$ , that is the initial three-body phase space, which also is responsible for the well defined limit of zero energy where  $\gamma \propto E^2$ . The usual recombination rate for zero energy is then found from Eq. (4) by letting  $E \rightarrow 0$ .

For absorption to take place the particles must cross or tunnel through the barrier and enter the region of finite imaginary potential. Barriers like in Fig. 1 may exhibit resonant behaviour around specific energies characterized by an abrupt change by  $\pi$  of the real part of the phase shift,  $\theta$ . A resonance, or bound state, may appear at zero energy with the corresponding scattering length denoted as  $a^{(-)}$ . At a resonance the probability for penetrating into the absorptive potential region is substantially increased. Consequently, the recombination rate is also substantially increased when three-body ( $E$ ) and resonance ( $E_0$ ) energies coincide.

This discussion in terms of scattering resonances strongly indicates that  $\alpha_{\text{rec}}$  can be parametrized by a Breit-Wigner distribution, that is

$$\alpha_{\text{rec}}(a, E) = \frac{4(2\pi)^2 3\sqrt{3}K}{[E - E_0(a)]^2 + \frac{1}{4}\Gamma^2(a)} \frac{\hbar^5}{m^3}, \quad (5)$$

where the numerical factor is chosen for easy comparison to Eq. (4). This expression exhibits the physical interpretation of tunnelling through the barrier and subsequently subject to absorption and reflection at short distance. The dimensionless constant  $K$  describes absorption and depends only on the imaginary potential.

We can give an alternative argument for the form of the recombination rate that is based on the WKB formulation which has been successfully used for few-body recombination in Refs. [36, 37]. The WKB tunneling probability for given energy,  $E$ , through the  $\nu^2/\rho^2$  barrier in Eq.(1) is easily calculated. We have here added the Langer correction effectively removing the term  $-1/4$

as required for a semi-classical calculation. The classical turning points are then  $\rho = 2/\sqrt{2mE/\hbar^2}$  and  $\rho \approx a$ , where we use the large-distance limit of  $\nu = 2$  and that the potential strongly decreases inside the barrier. The corresponding probability depends on  $\exp(-2S) \propto E^2 a^4$  (with  $S$  is the action integral [37]), and scales precisely with  $E^2$  where the power of 2 is directly related to the large  $\rho$  limit with  $\nu = 2$ . This is dictated by the three-body phase space dependence on energy. The second order WKB expression is  $1/(1 + \exp(2S))$  [38] which improves the first order WKB,  $\exp(-2S)$ , when  $S$  approaches zero for energies close to the barrier height. Thus, the WKB tunnelling approximation also leads to the Breit-Wigner parametrization in Eq. (5). The resonance position cannot, however, be determined from barrier properties.

Combining cross section, tunneling probability, and absorption potential yields an interpretation in terms of a two-step process; tunneling at large distance followed by absorption/reflection at short distance. When the barrier is negligible compared to the energy, all resonance structures are completely smeared out. Furthermore, as seen from Eq. (5), the recombination rate reaches an upper bound inversely proportional to the energy. This is known as the unitarity limit [39].

The objective is now to determine the parameters,  $\rho_{\text{imag}}$  and  $V_{\text{imag}}$ , of the imaginary potential, preferentially to fit experimental data by full numerical calculation. In general  $\rho_{\text{imag}}$  sets the location of recombination peaks as function of scattering length while  $V_{\text{imag}}$  determines the overall shape of these peaks. Both parameters are short-range parameters reflecting that recombination requires all three particles to be close to each other for recombination to occur. However, the final states are bound dimers with one free particle. In fact, it has recently been argued that the short-range three-body cut-off is determined by the short-range two-body repulsion. That argument involves the threshold for the appearance of the first Efimov three-body state out of the three-atom continuum [25]. While this point is typically determined by recombination loss peaks, previous theoretical models have only discussed the spectrum and not the loss.

The next step in the parametrization is to find  $K$ ,  $E_0$ , and  $\Gamma$ . The choice of factors in Eq. (5) immediately gives the high-energy limit,  $K \rightarrow 1 - \exp(-4\gamma)$ , where  $E$  has to be large compared to other terms in the denominator of Eq. (5). The peaks appearing when  $a = a^{(-)}$  at intervals of  $\exp(\pi/s_0) \approx 22.7$  ( $s_0 = 1.00624$ ) require corresponding periodicity. Both  $\Gamma$  and  $E_0$  can be parametrized by

$$\Gamma^2(a) \frac{m^2 a^4}{\hbar^4} = A \sin^2 \left[ s_0 \ln \left( \frac{a}{a^{(-)}} \right) \right] + \delta, \quad (6)$$

$$E_0(a) \frac{m a^2}{\hbar^2} = B \sin \left[ s_0 \ln \left( \frac{a}{a^{(-)}} \right) \right] + \beta, \quad (7)$$

where  $A, B, \beta, \delta$  are constants that weakly depend on the imaginary potential. This form ensures that both

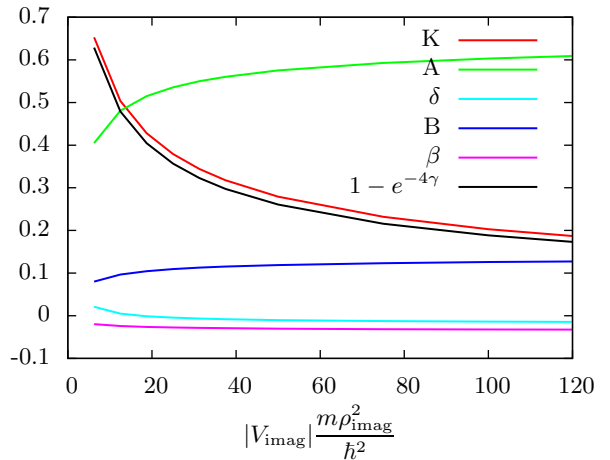


Fig. 2: The parameters of Eqs. (6) and (7) as functions of the strength of the imaginary square-well potential. All quantities are dimensionless.

the  $a^4$ -rule and the Efimov scaling are obeyed with periodic 22.7 peak-recurrence for given  $a = a^{(-)}$ . In Fig. 2 we plot the parameters for each imaginary strength,  $|V_{\text{imag}}| m \rho_{\text{imag}}^2 / \hbar^2$ , obtained by fitting Eqs. (5), (6), and (7) at finite energy to the numerical calculation from Eq. (4). We see that  $B$  is much smaller than  $A$  meaning that  $E_0$  is of little significance compared to  $\Gamma$ . The variables  $\beta$  and  $\delta$  are also insignificant, at least a factor of 10 smaller than  $A$  and  $B$ . The low-energy dependence of  $\alpha_{\text{rec}}$  on energy is thus primarily determined by  $K/\Gamma^2$ . The variations with imaginary strength between 10 and 120 amount to only about 10 – 20 %, except for  $K$  which decrease by about a factor of 2. As we will see below, experimental constraints limit the imaginary strength variation interval to  $\sim 10 - 25$ .

Experiments are performed at finite temperature, as opposed to finite energy. We therefore average the finite energy calculations using a normalized Boltzmann distribution for three particles, that is

$$\langle \alpha_{\text{rec}}(a) \rangle_T = \frac{1}{2(k_B T)^3} \int E^2 e^{-E/k_B T} \alpha_{\text{rec}}(a, E) dE, \quad (8)$$

where  $E^2$  arises due to the phase space for three particles. The effect of temperature was previously considered in other works such as Refs. [39] and [40]. With the parametrized expression in Eq. (5) this folding can readily be achieved. In the high temperature limit,  $T \gg \Gamma$ , where only large energies contribute  $\langle \alpha_{\text{rec}}(a) \rangle_T \approx \alpha_{\text{rec}}(a, E = T\sqrt{2})$ . The opposite limit of very small  $T$  naturally leads to  $\langle \alpha_{\text{rec}}(a) \rangle_T \approx \alpha_{\text{rec}}(a, E \approx 0)$ .

We now compare experimental data and numerical calculations with our imaginary potential. Full numerical results and the parametrization are virtually indistinguishable. The experimental recombination data for  ${}^7\text{Li}$  [23] along with calculations from our model at zero

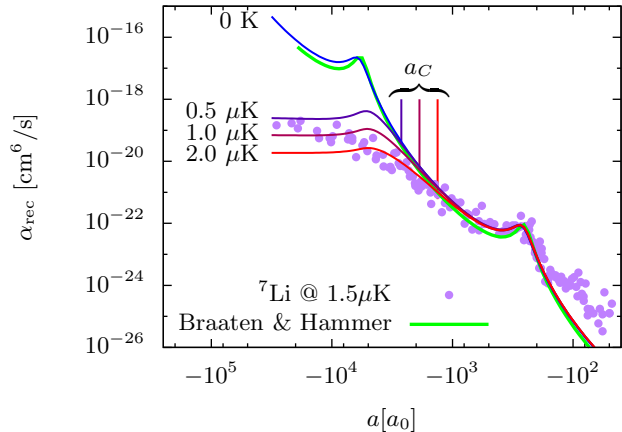


Fig. 3: Recombination coefficient  $\alpha_{\text{rec}}$  at zero and finite temperature (in  $\mu\text{K}$ ) for  ${}^7\text{Li}$  with experimental data at a temperature of  $1.5\mu\text{K}$  [23]. The scattering length,  $a$ , is in units of the Bohr radius,  $a_0$ .  $a_C$  indicates the critical scattering length where the height of the barrier equals the mean energy of the atoms. At this value the spectrum starts to deviate from the  $a^4$  behaviour.

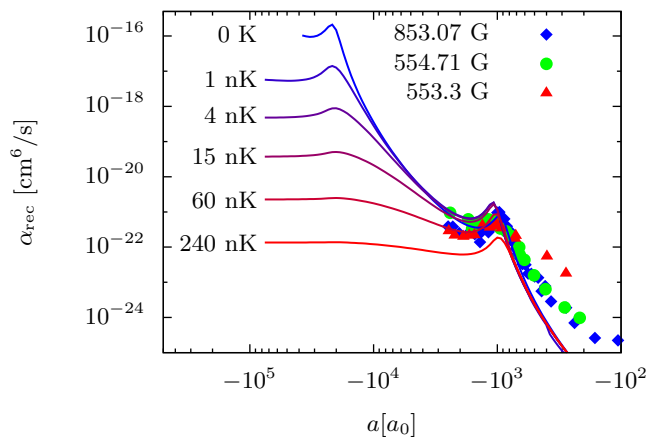


Fig. 4: Recombination coefficient  $\alpha_{\text{rec}}$  at zero and finite temperature for  ${}^{133}\text{Cs}$  with experimental data taken at a temperature of about  $15\text{ nK}$  [25].

and finite temperature is shown in Fig. 3. The only pronounced measured peak at  $a \approx -280a_0$  (where  $a_0$  is the Bohr radius) is well described by our model. The peak position is fitted with  $\rho_{\text{imag}} = 0.41a_0$  and the overall shape of the peak is fitted with  $V_{\text{imag}} = -68\hbar^2/ma_0^2$ . For zero temperature we find for all  $a$  almost precisely the same as the zero-energy formula of Ref. [4] where  $\eta^- = 0.12$  and  $a^{(-)} = -241a_0$  [23]. At finite temperature, we find the observed lowering of recombination rates for large  $a$ . This flattening of  $\alpha_{\text{rec}}$  appears for temperatures exceeding the barrier height, in other words for  $a^2 > a_C^2 \equiv 0.143\hbar^2a_0^2/(mTk_B)$  as is shown in Fig. 3 for the temperatures indicated. Recombination rates are

also measured for  ${}^{133}\text{Cs}$  at  $T \sim 15\text{ nK}$  for three different Feshbach resonances [25] which show very similar behavior. These are shown in Fig. 4 along with our calculations for different temperatures using  $\rho_{\text{imag}} = 1.58a_0$  and  $V_{\text{imag}} = -10\hbar^2/ma_0^2$ . Our model reproduces the data for all three resonances with the same model parameters. No data exists at  $-2 \times 10^4 a_0$  where we predict another peak. From Fig. 4 we conclude that a temperature below  $\sim 2\text{ nK}$  seems to be required to observe this peak.

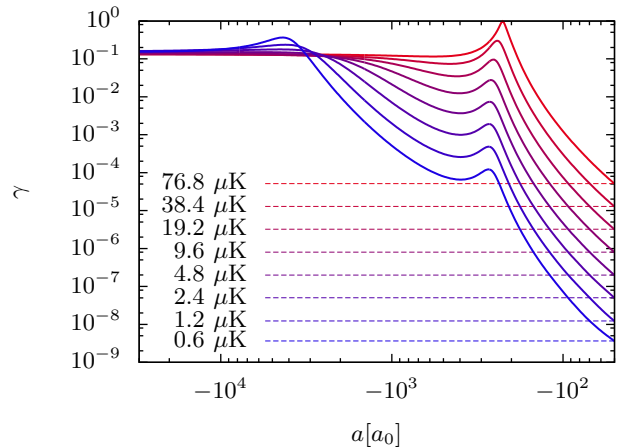


Fig. 5: The decay parameter  $\gamma$  for the  ${}^7\text{Li}$  system as a function of scattering length for finite energies in temperature units. At high  $|a|$  all curves have about the same value  $\sim 0.14$ , independent of energy.

Increasing  $|a|$  moves the barrier towards infinity and reduces  $E_B(a)$ , which is thus exceeded by typical laboratory temperatures. This means that the high-energy limit is approached and an  $a$ -independent recombination rate is obtained. The energy dependence in this limit is  $1/E^2$  and the value of  $K$  determines the limiting value of  $\alpha_{\text{rec}}$ . We show in Fig. 5 the calculated values of  $\gamma$  as a function of  $a$  for several finite energies. All  $\gamma$ -values are lowered but for large  $|a|$  an energy and  $a$  independent constant of  $\approx 0.14$  is reached. This value depends on the strength of the imaginary potential  $mV_{\text{imag}}\rho_{\text{imag}}^2/\hbar^2$ , which controls the height and shape of the absorption as function of both  $E$  and  $a$ . This value is numerically deceptively similar to the  $\eta^-$  of [23] used to fit the peak in Fig. 3. Formally there is also a connection although  $\eta^-$  is more complicated and derived through multiple scattering theory for zero energy [4]. The physical meaning is different from our  $\gamma$  and the expressions are not one-to-one related.

In conclusion, we present a simple and physically transparent model of three-body recombination for negative scattering lengths that does not require a short-range three-body cut-off. Instead it includes an imaginary potential at short distance that takes decay into deeply bound dimers into account. Full numerical solution of the three-body equations were used to obtain the re-

combination rate and subsequently a parametrization in terms of the Breit-Wigner resonance formula was presented and shown to display the expected scaling behavior. Finally we showed how this new model reproduces experimental data on  ${}^7\text{Li}$  and  ${}^{133}\text{Cs}$ . If we express the radius of the imaginary potential in units of the van der Waals length we find  $\rho_{\text{imag}}/r_{\text{vdW}} = 0.0063$  and  $\rho_{\text{imag}}/r_{\text{vdW}} = 0.0078$  respectively, while the strength is  $|V_{\text{imag}}|/V_{\text{vdW}} = 2.87 \cdot 10^5$  and  $|V_{\text{imag}}|/V_{\text{vdW}} = 4.08 \cdot 10^5$  where  $V_{\text{vdW}} = \hbar^2/mr_{\text{vdW}}^2$ . The similarity of  $\rho_{\text{imag}}$  and  $V_{\text{imag}}$  in van der Waals units indicates that there could be universality hidden in this parameter. The differences that we find is most likely related to the difference in deeply bound state in the two-body potentials of  ${}^7\text{Li}$  and  ${}^{133}\text{Cs}$ . Further studies using models that include realistic potentials for the deep dimers are needed to fix the parameters of our model to state-of-the-art short-range calculations and data.

- 
- [1] V. Efimov, *Yad. Fiz* **12**, 1080 (1970); *Sov. J. Nucl. Phys.* **12**, 589 (1971).
- [2] E. Nielsen, D. V. Fedorov, A. S. Jensen, and E. Garrido, *Phys. Rep.* **347**, 373 (2001).
- [3] A. S. Jensen, K. Riisager, D. V. Fedorov, and E. Garrido, *Rev. Mod. Phys.* **76**, 215 (2004).
- [4] E. Braaten and H. W. Hammer, *Phys. Rep.* **428**, 259 (2006).
- [5] T. Kraemer *et al.*, *Nature* **440**, 315 (2006).
- [6] C. Chin, R. Grimm, P. S. Julienne, and E. Tiesinga, *Rev. Mod. Phys.* **82**, 1225 (2010).
- [7] F. Ferlaino and R. Grimm, *Physics* **3**, 9 (2010).
- [8] T. B. Ottenstein, T. Lompe, M. Kohnen, A. N. Wenz, and S. Jochim, *Phys. Rev. Lett.* **101**, 203202 (2008).
- [9] S. E. Pollack, D. Dries, and R. G. Hulet, *Science* **326**, 1683 (2009).
- [10] M. Zaccanti *et al.*, *Nature Phys.* **5**, 586 (2009).
- [11] N. Gross, Z. Shotan, S. Kokkelmans, and L. Khaykovich, *Phys. Rev. Lett.* **103**, 163202 (2009).
- [12] J. H. Huckans, J. R. Williams, E. L. Hazlett, R. W. Stites, and K. M. O'Hara, *Phys. Rev. Lett.* **102**, 165302 (2009).
- [13] J. R. Williams, E. L. Hazlett, J. H. Huckans, R. W. Stites, Y. Zhang, and K. M. O'Hara, *Phys. Rev. Lett.* **103**, 130404 (2009).
- [14] T. Lompe, T. B. Ottenstein, F. Serwane, A. N. Wenz, G. Zürn, and S. Jochim, *Science* **330**, 940 (2010).
- [15] N. Gross, Z. Shotan, S. Kokkelmans, and L. Khaykovich, *Phys. Rev. Lett.* **105**, 103203 (2010).
- [16] T. Lompe, T. B. Ottenstein, F. Serwane, K. Viering, A. N. Wenz, G. Zürn, and S. Jochim, *Phys. Rev. Lett.* **105**, 103201 (2010).
- [17] S. Nakajima, M. Horikoshi, T. Mukaiyama, P. Naidon, and M. Ueda, *Phys. Rev. Lett.* **105**, 023201 (2010).
- [18] S. Nakajima, M. Horikoshi, T. Mukaiyama, P. Naidon, and M. Ueda, *Phys. Rev. Lett.* **106**, 143201 (2011).
- [19] R. J. Wild, P. Makotyn, J. M. Pino, E. A. Cornell, and D. S. Jin, *Phys. Rev. Lett.* **108**, 145305 (2012).
- [20] O. Machtey, D. A. Kessler, and L. Khaykovich, *Phys. Rev. Lett.* **108**, 130403 (2012).
- [21] O. Machtey, Z. Shotan, N. Gross, and L. Khaykovich, *Phys. Rev. Lett.* **108**, 210406 (2012).
- [22] S. Knoop, J. S. Borbely, W. Vassen, S. J. J. M. F. Kokkelmans, *Phys. Rev. A* **86**, 062705 (2012).
- [23] P. Dyke, S. E. Pollack, and R. G. Hulet, arXiv:1302.0281 (2013).
- [24] S. Roy *et al.*, arXiv:1303.3843.
- [25] M. Berninger *et al.*, *Phys. Rev. Lett.* **107**, 120401 (2011).
- [26] P. Naidon, E. Hiyama, and M. Ueda, *Phys. Rev. A* **86**, 012502 (2012).
- [27] C. Chin, arXiv:1111.1484v2.
- [28] J. Wang, J. P. D'Incao, B. D. Esry, and C. H. Greene, *Phys. Rev. Lett.* **108**, 263001 (2012).
- [29] P. K. Sørensen, D. V. Fedorov, A. S. Jensen, and N. T. Zinner, *Phys. Rev. A* **86** 052516 (2012).
- [30] R. Schmidt, S. P. Nath, and W. Zwerger, *Eur. Phys. J. B* **85**, 386 (2012).
- [31] P. Naidon, S. Endo, and M. Ueda, arXiv:1208.3912.
- [32] E. Nielsen and J. H. Macek, *Phys. Rev. Lett.* **83**, 1566 (1999).
- [33] B. D. Esry, C. H. Greene, and J. P. Burke, *Phys. Rev. Lett.* **83**, 1751 (1999).
- [34] P. F. Bedaque, E. Braaten, and H.-W. Hammer, *Phys. Rev. Lett.* **85**, 908 (2000).
- [35] E. Braaten and H.-W. Hammer, *Phys. Rev. Lett.* **87**, 160407 (2001).
- [36] P. K. Sørensen, D. V. Fedorov, and A. S. Jensen, *Few-Body Syst.* **54**, 579 (2013).
- [37] P. K. Sørensen, D. V. Fedorov, A. S. Jensen, and N. T. Zinner, *J. Phys. B: At. Mol. Opt. Phys.* **46**, 075301 (2013).
- [38] N. Fröman and P. O. Fröman, *Physical Problems Solved by the Phase-Integral Method* (Cambridge University Press, UK, 2002).
- [39] J. P. D'Incao, H. Suno, and B. D. Esry, *Phys. Rev. Lett.* **93**, 123201 (2004).
- [40] E. Braaten, H.-W. Hammer, D. Kang, and L. Platter, *Phys. Rev. A* **78**, 043605 (2008).